Is the inverted field gradient in the Catalina Schist Terrane primary or constructional?

John P. Platt[1] and William L. Schmidt[1],

[1]Department of Earth Sciences, University of California, Los Angeles, CA, USA.

Correspondence to: John P. Platt

jplatt@usc.edu

Key points:

- New geothermometry shows that high-pressure rocks on Catalina define an inverted metamorphic temperature zonation
- The zonation is disrupted, and the present structure does not represent an original inverted thermal gradient
- The zonation formed by progressive underplating in a cooling subduction zone following a high-T metamorphic event

Index Terms:

3613 Subduction zone processes

3660 Metamorphic petrology

3651 Thermobarometry

Key words:

Laser Raman Spectroscopy

Carbonaceous material

Inverted thermal gradient

High-pressure low-temperature metamorphism

Underplating

Subduction channel

Abstract

New geothermometry using laser-Raman data on carbonaceous material from low and intermediate grade rocks on Santa Catalina Island, California, together with existing thermobarometric data, show that there is a quasi-continuous increase in peak metamorphic temperature from 327 ± 8°C in lawsonite blueschist facies rocks at the lowest structural levels, through ~ 433°C in overlying epidote blueschists, 546 ± 20°C in albite-epidote amphibolite facies rocks, to 650-730°C in amphibolite facies rocks at the top of the sequence. Rocks of different metamorphic grade are separated from one another by tectonic contacts across which temperature increases by ~100°C in each case. Previously published geochronological data indicate that peak metamorphism in the highest grade rocks at 115 Ma preceded deposition of blueschist facies metasediments by ~ 15 million years, so that the present inverted grade sequence does not represent an original inverted temperature gradient. The present structure results from progressive underplating of oceanic rocks in a cooling subduction zone following a high-T metamorphic event at 115 Ma. An inverted temperature gradient of ≥100°C/km across the subduction channel likely existed during the high-T event, decreased during underplating, and reached zero by ~90 Ma.

1. Introduction.

The Catalina Schist terrane is an assemblage of high-pressure low-temperature metamorphic rocks that is generally accepted to form part of the Franciscan accretionary complex, created by Mesozoic/Early Tertiary subduction of oceanic lithosphere beneath the western Laurentian margin during Mesozoic time. It is anomalous in several respects, however; most notably in the presence of a body several square km in extent of upper amphibolite facies rocks associated with serpentinized harzburgite at the top of the complex. These rocks, together with underlying rocks of lower metamorphic grade, have been cited as an example of an inverted metamorphic gradient [e.g., *Platt*, 1975; *Graham and England*, 1976; *Platt*, 1986; *Peacock*, 1987], possibly analogous to those developed beneath ophiolite complexes in Newfoundland, Oman, and elsewhere [e.g., *Jamieson*, 1980; *Searle and Malpas*, 1980]. The origin of inverted metamorphic sequences has been extensively debated, and is variously ascribed to conductive heat transfer from a hot upper plate, such as young ocean lithosphere in the hanging wall of a subduction zone [e.g., *Platt*,

1975; *Peacock*, 1987; *Wakabayashi*, 1990; *Mosenfelder and Hacker*, 1996], shear heating along the subduction zone interface [*England and Molnar*, 1993; *England & Smye*, 2023], progressive underplating in a cooling environment [*Soret et al.*, 2017], or folding and thrust imbrication of a previously normal metamorphic sequence during exhumation [*Searle et al.*, 1999; *Vannay and Grasemann*, 2001].

Bailey [1941] originally recognized the presence of the high-grade rocks on Catalina, and described them as being in thrust contact with lower grade schists that he referred to as Franciscan. *Platt* [1975]; [1976] showed that rocks of intermediate metamorphic grade, which he referred to as the Greenschist Unit, are in tectonic contact above blueschist facies rocks (the Blueschist Unit), and both are tectonically overlain by the high-grade rocks (Amphibolite Unit). *Grove and Bebout* [1995] subsequently showed that the intermediate grade rocks include slices of epidote blueschist and albite-epidote amphibolite grade, and *Grove et al.* [2008] suggested that some of the rocks at the lowest structural levels lack glaucophane and hence belong the the lawsonite-albite facies. Precise determinations of the P-T conditions in these different rock units have been lacking, however, primarily because of the lack of appropriate geothermometers. In this paper we present peak temperature determinations based on laser-Raman data on carbonaceous material (LRCM) from the low and intermediate grade rocks in the Catalina Schist, and integrate these with previously published thermobarometric and geochronological data. We show that although the rocks of different metamorphic grade are largely separated from each other by tectonic contacts, overall they constitute a quasi-continuous inverted metamorphic sequence. We discuss to what extent this could represent the disrupted remnants of a primary inverted grade sequence, or whether it is a product of later tectonic processes.

2. Tectonic setting of the Catalina Schist.

Present-day exposures of the Catalina Schist are limited to Santa Catalina Island itself and some very limited exposures on the Palos Verdes peninsula, south of Los Angeles (Figure 1). Clasts derived from the Catalina schist are widespread in the early to middle Miocene San Onofre breccia, however, which is widely exposed along the coast of southern California and on the northern Channel Islands [*Stuart*, 1979]. This suggests that the schist underlies much of the Inner Continental Borderland of southern California [*Howell and Vedder*, 1981]. The presence of high-pressure low-temperature metamorphic rocks (lawsonite and epidote blueschists) within

the terrane, and their lithological and petrological similarity to rocks in the eastern belt of the Franciscan Complex of the northern and central Coast Ranges of California, has led to general acceptance that the terrane forms part of, or is closely related to, the Franciscan Complex. As discussed below, however, the higher grade rocks on Catalina are distinct both in metamorphic grade and the timing of peak metamorphism.

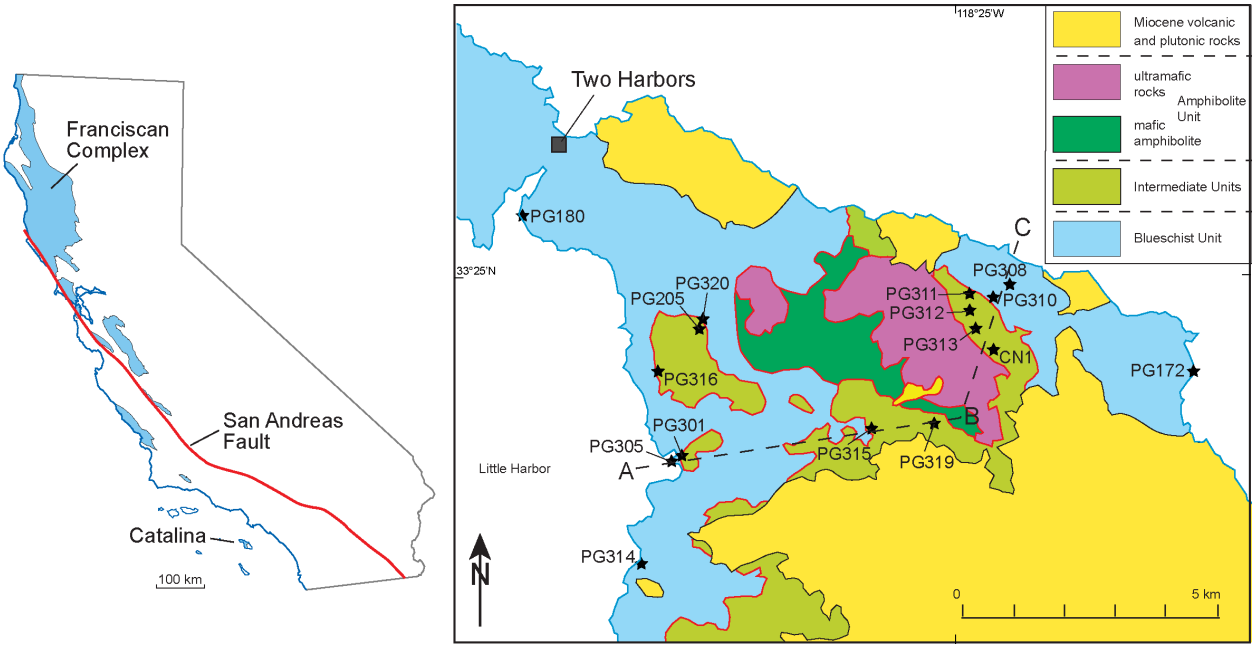

Figure 1. Left: outline of California, showing the Franciscan Complex, the San Andreas Fault, and the location of Santa Catalina Island. Right: map of central Catalina Island, after *Platt* [1975], showing the main tectonic units, the location of samples, and the section line ABC shown in Figure 2.

The metamorphic rocks on Catalina Island vary in grade from lawsonite-albite to upper amphibolite facies (Figures 1 and 2), which has led to widely varying suggestions of their relationships and origins. The structurally lowest rocks in the central part of the island are in the lawsonite blueschist facies. Mafic schists carry glaucophane + lawsonite + sphene, and metagraywackes carry quartz +white mica + chlorite + lawsonite ± glaucophane ± jadeitic pyroxene. Some undeformed metabasalts (pillow lava and pillow breccia with diabase dikes) contain omphacite replacing primary augite, in addition to glaucophane and lawsonite; and some metagraywackes contain veins and small porphyroblasts of albite, which may have formed during exhumation and decompression. Stilpnomelane is widespread in all rock types. On the northwestern end of the island, the lithological assemblage is very similar (metagraywacke,

metabasalt, and metachert), but sodic amphibole is less abundant, and these rocks have been attributed to the lawsonite-albite facies [*Grove et al.*, 2008]. It is unclear whether these rocks are separated from the lawsonite blueschists by a grade boundary or a tectonic contact.

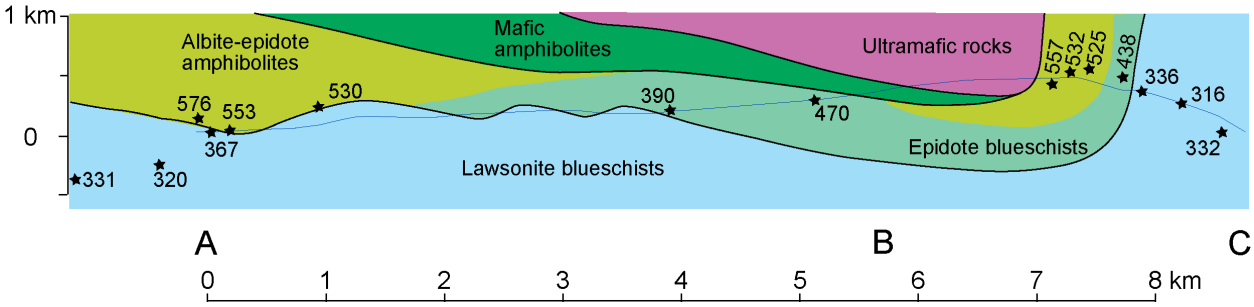

Figure 2. Structural section ABC across central Catalina Island with LRCM temperatures in °C (for location see Figure 1). Stars show sample locations. Locations not on the topographic profile (pale blue line) have been projected in laterally (see Figure 1), and are subject to some uncertainty in position.

In the central part of the island the lawsonite blueschists are overlain by rocks of variable but intermediate grade, which were grouped together by *Platt* [1975] as the Greenschist Unit. These rocks largely lack primary textures, and show strong deformational fabrics, but the protoliths appear to have been similar to those of the underlying lawsonite blueschists; greywacke sandstone and shale, basalt, and chert. Pillow structures are locally preserved in the metabasalts. *Grove and Bebout* [1995] showed that in different outcrop areas these rocks are best described as either epidote blueschists or epidote amphibolites. They all contain clinozoisite or epidote rather than lawsonite, but the dominant amphibole is variously glaucophane, actinolite, or hornblende. Calcic and sodic amphibole are commonly closely associated in the epidote blueschists, even in the same thin section, without evidence for replacement of one by the other. Metasedimentary rocks contain quartz + albite + clinozoisite + white mica ± actinolite ± biotite ± garnet. Chlorite commonly forms pseudomorphs after biotite and garnet. Metacherts may contain garnet, sodic amphibole, and either stilpnomelane or biotite. Sodic amphibole appears to coexist with biotite and garnet in some of the metachert from the albite-epidote amphibolite facies rocks.

Rocks of intermediate grade are always separated from the underlying lawsonite blueschists by a tectonic contact, which is commonly occupied by a mélange unit consisting of meta-somatized ultramafic rock (predominantly either serpentinite or talc + actinolite + chlorite), with

tectonic blocks, primarily of high-grade rocks very similar to those in the ultramafic mélange of the Amphibolite Unit. Tectonic boundaries between intermediate slices of different grade have not been identified, and there is no evidence that they are separated by mélange. On the NE side of the island, no mélange unit separates the lawsonite blueschists from the intermediate grade rocks, and the grade change appears to be abrupt.

The highest grade rocks on Catalina (Amphibolite Unit) lie in tectonic contact on all the underlying rocks. The contact is generally quite sharp, and marked by a narrow zone of metasomatized ultramafic rock with some tectonic blocks [*Harvey et al.*, 2020]. The lower part of the Amphibolite Unit consists of a large body of coherent mafic amphibolite, with pale green hornblende + zoisite/clinozoisite + plagioclase ± diopside. The plagioclase originally had an intermediate composition, but has largely been retrogressed to fine-grained sodic plagioclase + zoisite + white mica. Thin layers with garnet and dark hornblende rich in Fe and Ti are locally present. The entire body has a strong deformational fabric, lacks primary textures, and shows evidence of partial melting during metamorphism [*Sorensen and Barton*, 1987]. The Mg-rich bulk composition, and the presence of a consistent compositional layering, suggests that it may represent a body of cumulate gabbro [*Platt*, 1976]. The mafic amphibolite is overlain by metasedimentary rocks, comprising coherent (but strongly deformed) migmatitic paragneiss and quartzite. The paragneiss is made up of quartz + plagioclase + muscovite + biotite + garnet ± kyanite ± zoisite/clinozoisite ± rutile. Quartzite is generally very coarse-grained, but contains trains of fine-grained garnet, as well as trace amounts of rutile and zircon [*Page et al.*, 2019; *Harvey et al.*, 2020]. It is likely to be metachert.

These rock bodies are overlain by two contrasting bodies of ultramafic rock. Massive serpentinized spinel harzburgite occurs as a km-scale coherent body directly overlying coherent mafic amphibolite in the west of the area, and elsewhere as blocks in ultramafic mélange. The latter forms a large body discordantly overlying the coherent mafic amphibolite and the metasedimentary rocks. The mélange matrix is schistose with variable amounts of serpentine, talc, chlorite, and both calcic and Mg-amphiboles. The matrix encloses blocks up to tens of m in extent, primarily of garnet hornblendite, with smaller amounts of massive serpentinite, metasedimentary rocks, and quartz-plagioclase pegmatite. All components of the mélange show evidence of upper amphibolite-facies metamorphism.

A more detailed discussion of published thermobarometric and geochronological data from the various elements in the Catalina Schist follows our presentation of the LRCM data.

3. LRCM methods.

Samples were collected with the aim of obtaining enough carbonaceous material (CM) to carry out laser Raman analysis, with a focus on carbonaceous metasediments. All samples were cut perpendicular to foliation and, where a lineation was present, parallel to the lineation. Raman spectroscopy of CM was carried out at the Natural History Museum of Los Angeles using a Jorbin Technology/Horiba Instruments Xplora Plus Raman Microscope with a 532 nm laser, 2400 lines/mm diffraction grating, and a laser power at the sample surface of ~1.7 mW. Each measurement consisted of five accumulations of 30 seconds per accumulation. All analysis points were selected to be slightly below the surface of the thin section, to avoid analyzing CM damaged by polishing [*Pasteris*, 1989; *Beyssac et al.*, 2003; *Ammar and Rouzaud*, 2012; *Lünsdorf*, 2016; *Henry et al.*, 2018]. Spectra were qualitatively assessed for temperature range based on Figure 2 in *Kouketsu et al.* [2014] and then curve fitting and temperature determination were done following the procedures described in *Kouketsu et al.* [2014] for samples between 150 – 400°C, while the procedures described in [*Beyssac et al.*, 2002] were used for samples qualitatively determined to be >400°C. *Kouketsu et al.* [2014] define the Raman temperature as:

$$T(°C) = -2.15\ x\ \mathrm{FWHM_{D1}} + 478 \qquad (1)$$

Where $\mathrm{FWHM_{D1}}$ is equal to the full width at half maximum of the D1 band. *Beyssac et al.* [2002] define the Raman temperature as:

$$T(°C) = -445(R2) + 641 \qquad (2)$$

Where R2 is equal to the peak area ratio D1/(G + D1 + D2). For a full discussion on FWHM and the R2 ratio see *Kouketsu et al.* [2014] and *Beyssac et al.* [2002] respectively. A minimum of 12 analyses were performed per sample and the results were averaged to obtain a temperature for the sample. Peaks were deconvolved using the computer program PeakFit 4.12 (SeaSolve Software Inc.). Absolute error for Raman analysis is typically taken as ~50°C [e.g., *Beyssac et*

166 *al.*, 2002]. Errors reported in this paper are measurement errors, reported at 1σ based on ~12
167 measurements per sample. For a review on the use of LRCM in determining metamorphic
168 temperatures, see *Henry et al.* [2019].

169 **4. LRCM results.**

170 We present LRCM data from 15 samples of metamorphosed carbonaceous shale from the
171 blueschist and intermediate units on central Catalina Island (Table 1). The locations of the data
172 are shown on the geologic map (Figure 1) and the temperatures are shown on the synthetic cross-
173 section (Figure 2). Representative Raman spectra for each sample are shown in Figure 3.

Sample	Unit	GPS	n	Average R2	$FWHM_{D1}$	T (°C)
CN1	Ab-ep amph	N33° 24.333' W118° 24.454	12	0.19 ± 0.08	-	557 ± 36
PG172	Laws bs	N33° 23.996' W118° 22.055	12	-	68 ± 12	332 ± 26
PG180	Laws bs	N33° 25.578' W118° 30.352	12	-	68 ± 10	331 ± 21
PG301	Ab-ep amph	N33° 23.159' W118° 28.443	13	0.20 ± 0.11		553 ± 50
PG305	Laws bs	N33° 23.111' W118° 28.462	12	-	52 ± 3	367 ± 6
PG308	Laws bs	N33° 24.868' W118° 24.398	12	-	75 ± 3	316 ± 7
PG310	Laws bs	N33° 24.791' W118° 24.553	13	-	66 ± 12	337 ± 25
PG311	Ep bs	N33° 24.800' W118° 24.728	12	0.46 ± 0.05	-	438 ± 21
PG312	Ab-ep amph	N33° 24.691' W118° 24.743	12	0.26 ± 0.06	-	525 ± 26
PG313	Ab-ep amph	N33° 24.470' W118° 24.726	12	0.24 ± 0.09	-	532 ± 41
PG314	Laws bs	N33° 22.010' W118° 22.055	12	-	74 ± 7	320 ± 16
PG315	Ep bs	N33° 23.442' W118° 26.084	12	-	41 ± 2	390 ± 3
PG316	Ab-ep amph	N33° 24.012' W118° 28.663	12	0.15 ± 0.05	-	576 ± 25
PG319	Ep bs	N33° 23.512' W118° 25.276	12	0.39 ± 0.06	-	470 ± 26
PG320	Ab-ep amph	N33° 24.445' W118° 28.193	12	0.25 ± 0.08	-	530 ± 37

Statistics	mean	s.d.	
Laws bs	333.8	15.4	
	327.2	8.8	Excluding PG305
Ep bs	432.7		
Ab-ep amph	545.5	19.8	

174

175 *Table 1*. Raman data. Unit abbreviations: Laws bs, lawsonite blueschist; Ep bs, epidote blueschist; Ab-
176 ep amp, albite epidote amphibolite. n = number of analyses, R2 = peak ratio, FWHM = full width half
177 maximum; T, temperature; s.d., standard deviation.

178

179 Six samples come from the Blueschist Unit at Catalina Harbor, Little Harbor, and Ben
180 Weston Beach on the west side of the island, and from the coast and canyons on the northeast
181 side. The other nine samples come from the slices of intermediate grade. Two are from the body
182 of epidote blueschists in Cottonwood Canyon, and a third from the epidote blueschists on the
183 northeast side of the island. Three samples come from the albite-epidote amphibolite facies

klippen in Little Springs Canyon and around Little Harbor, and the remaining three from greenschist or albite-epidote amphibolite facies rocks on the northeast side of the island.

The six Blueschist Unit samples yielded temperatures ranging from 316 – 367°C, with an average of 338 ± 16°C. The 367°C result, however, is an outlier: the remaining five samples average 327 ± 8°C, and there is no evidence for regional variation. This may therefore be the best estimate for the overall temperature of metamorphism of the Blueschist Unit. The 367°C result comes from a mélange unit at Little Harbor, within a few meters of the contact with the overlying intermediate grade rocks, which may explain the anomalously high temperature.

The three epidote blueschist samples give temperatures of 390 – 470°C, with an average of 433°C. The lowest and highest temperatures come from the Cottonwood Canyon samples; the sample from the north side gives 438°C. The 80°C range is outside the uncertainties on the individual determinations, and suggests a real variation in the peak temperature in these rocks. They have been interpreted by *Sorensen* [1986] as representing a disequilibrium assemblage, caused by increasing temperature during metamorphism, and *Platt* [1976] suggested that there are transitions in grade within rocks showing these assemblages. These temperatures are distinctly higher than those in the underlying lawsonite blueschists, however, and the difference is outside the uncertainties on the measurements, consistent with the interpretation of *Platt* [1975] that they form a tectonically distinct body of rocks.

The six greenschist and albite-epidote amphibolite facies samples yielded temperatures in the range 525 – 576°C, with an average of 546 ± 20°C. There is no clear indication of regional variation. Their temperatures are higher than those in the epidote blueschists, and the difference is outside the uncertainties on the measurements, which confirms the interpretation of *Grove and Bebout* [1995] that the epidote blueschists and albite-epidote amphibolite facies rocks are petrologically and tectonically distinct.

Six of our samples come from the northeast side of the island, and span the lower grade rocks up to the contact with the ultramafic mélange in the Amphibolite Unit around the airport. The six samples constitute a transect through the structural sequence on the island, where it has been tilted into a steep orientation. It is striking that the LRCM peak temperatures increase almost monotonically up through this sequence (Figure 2), although there are jumps of ~100°C from the lawsonite blueschists to the epidote blueschists, and then from epidote blueschists to the greenschist/albite-epidote amphibolite facies rocks.

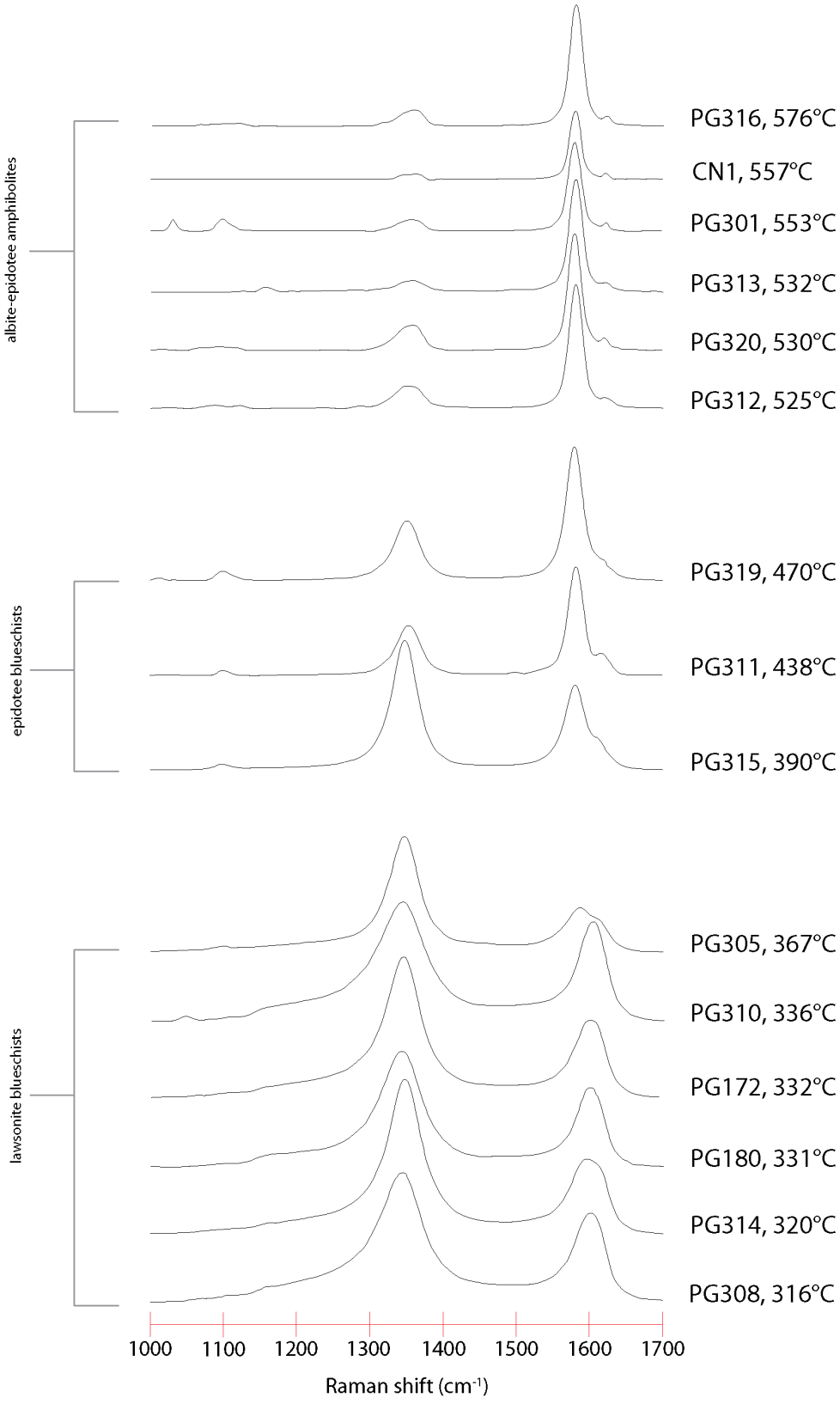

Figure 3. Representative Raman spectra.

5. Thermobarometric re-evaluation

Previous thermobarometric estimates from the low and intermediate grade rocks on Catalina are very qualitative, based on phase assemblages. The addition of quantitative temperature estimates allows us to determine more precise estimates of pressure from the stability fields of the minerals. In doing this, we have to take the following issues into account. First, the LRCM determinations are for the peak temperature, which is not necessarily reflected by the dominant mineral assemblage. Secondly, LRCM determinations, while fairly precise when used for comparing different samples, have a somewhat larger uncertainty when compared with geothermometry using other techniques. This stems from the fact that the various LRCM calibrations have been determined using metamorphic thermobarometry on specific sets of samples.

Metamorphic conditions in the Blueschist Unit were estimated by *Sorensen* [1986] at 300-400°C and 8-11 kbar. The mean LRCM peak temperature is 327 ± 8°C. The sporadic presence of jadeitic pyroxene in metagraywackes suggests that peak conditions were close to the albite → jadeite + quartz stability curve (Figure 4). The pyroxene is too fine-grained for accurate chemical analysis, but the average compositions of jadeitic pyroxene reported from blueschist-facies metagraywackes elsewhere in the Franciscan is typically > 82% jadeite [*Ernst*, 1965; *Newton and Smith*, 1967; *Ernst*, 1993; *Ernst and McLaughlin*, 2012], which has a stability limit only ~800 bars less than that of pure jadeite. On that basis we can refine the PT estimate to 327 ± 8°C and 10.6 ± 0.4 kbar.

Metamorphic conditions in the rocks attributed by *Platt* [1975] to the Greenschist Unit were estimated by *Sorensen* [1986] to lie in the range 450-550°C and 7-12 kbar. The epidote blueschists give the lowest LRCM peak temperatures, with an average of 433°C. At this temperature the stability of glaucophane constrains the minimum pressure to ~7 kbar, and the lack of jadeitic pyroxene places an upper limit to the pressure of ~13 kbar (Figure 4). This PT range lies entirely within the experimentally determined stability field of lawsonite, so it is striking that lawsonite has not been reported from these rocks, whereas they do contain clinozoisite or epidote as the main Ca-Al-bearing phase in both metasedimentary and metavolcanic rocks. The lack of lawsonite may therefore reflect a low water fugacity or a high oxygen fugacity, both of which might destabilize lawsonite relative to an epidote-group mineral close to the upper stability limit of lawsonite [*Tsujimori and Ernst*, 2014].

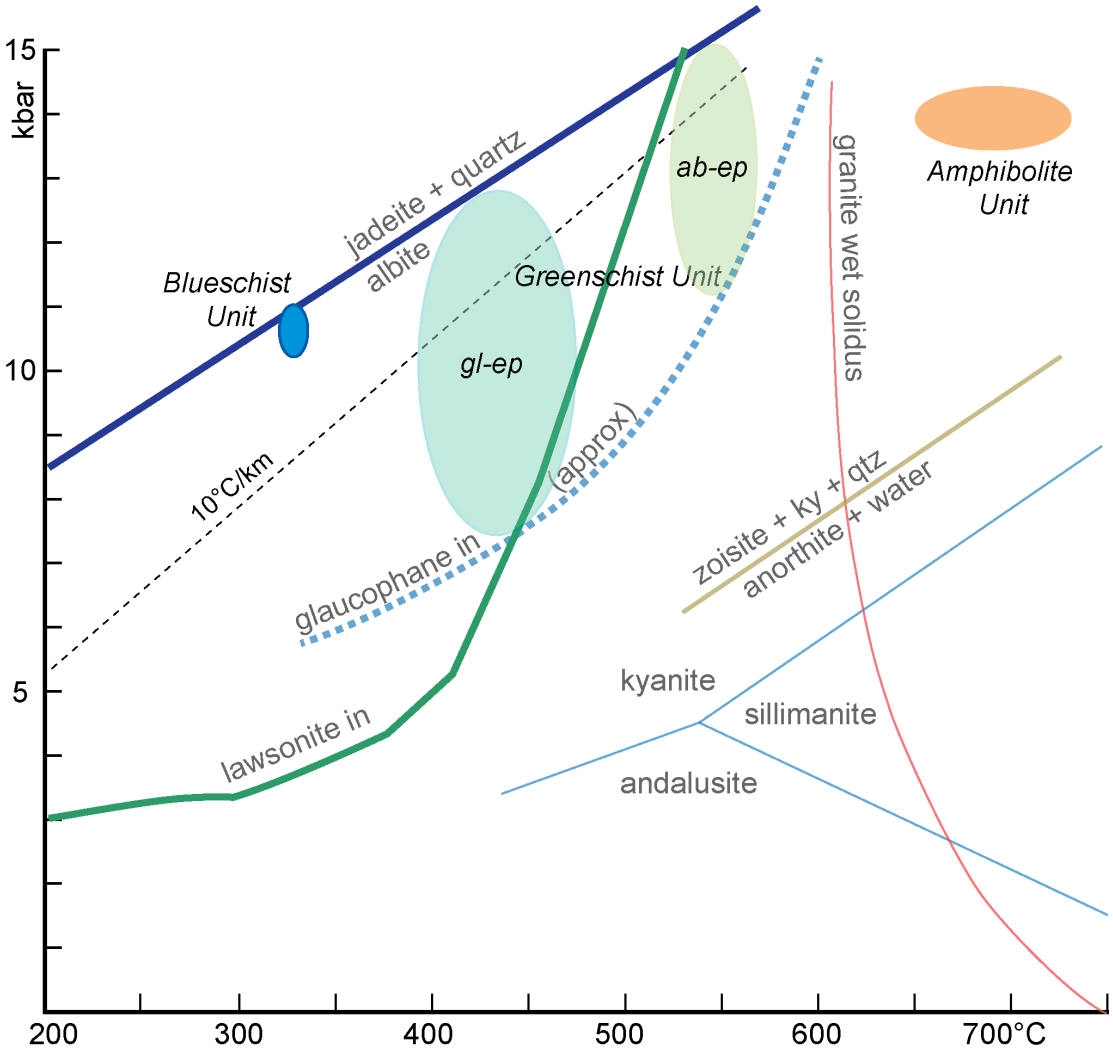

Figure 4. PT conditions of metamorphism in the various tectonic units on Catalina Island. Lower stability limit of lawsonite after *Liou* [1971]; glaucophane stability limit is very approximate, based on a discussion of the experimental data by *Tsujimori and Ernst* [2014]; breakdown of anorthite from *Newton and Kennedy* [1963]; breakdown of albite after *Newton and Smith* [1967]. gl-ep, epidote blueschist unit; ab-ep, albite-epidote amphibolite unit.

The greenschist to albite-epidote amphibolite facies rocks in the Greenschist Unit give a mean temperature of 546 ± 20°C, which is significantly higher than the range for the epidote blueschists. The presence of sodic amphibole in metacherts, and the lack of sodic pyroxene, constrain the pressure to between 11 and 15 kbar (Figure 4).

None of our LRCM estimates come from the Amphibolite Unit or the high-grade blocks on Catalina, but we summarize the thermobarometric information here, as it is relevant to the discussion of whether a primary inverted grade sequence existed. *Sorensen and Barton* [1987] and *Sorensen* [1988] estimated conditions in the Amphibolite Unit of 8-11 kbar and 640-750°C, based on mineral assemblages and the evidence for partial melting. *Penniston-Dorland et al.* [2018] subsequently determined temperatures of 650-730°C from the blocks in the ultramafic mélange using Zr in rutile thermometry, and *Harvey et al.* [2020] determined peak pressures of 13.4 –14.4 kbar from these blocks using quartz-in-garnet elastic barometry. *Dong et al.* [2022] suggested on the basis of lawsonite pseudomorphs enclosed in garnet from a high-grade block that it passed through the lawsonite-eclogite field at around 22 kbar, and was subsequently heated to ~ 800°C at 10 kbar during decompression. An early high-pressure history for the blocks is consistent with the local preservation of eclogite facies assemblages [*Platt et al.*, 2020]. For the purposes of this discussion we take the range 650-730°C and 13.4-14.4 kbar for the peak metamorphism of the Amphibolite Unit as a whole (Figure 4).

6. Geochronological constraints

Geochronology on low-grade metamorphic rocks is difficult, and the main constraints come from U-Pb dating of detrital zircon, which provides maximum depositional ages (MDAs) of clastic metasediments, and Ar-Ar dating of white micas, which in the lowest grade rocks are very fine-grained and commonly mixed with other sheet silicates. MDA from the lawsonite-blueschist facies metagraywackes is 97±3 Ma *Grove et al.* [2008], and Ar-Ar ages on white mica lie in the range 90-100 Ma [*Grove and Bebout*, 1995]. Taken together, these indicate deposition and subduction in a short period of time in the mid-Cretaceous (100-90 Ma).

Epidote blueschist facies metasediments give an MDA of 100±3 Ma [*Grove et al.*, 2008], and Ar-Ar ages on phengite are 95-99 Ma [*Grove and Bebout*, 1995]. These are indistinguishable within uncertainty from those in the lawsonite blueschists. The higher grade albite-epidote amphibolites, however, give an MDA of 113±3 Ma [*Grove et al.*, 2008], and Ar-Ar on phengite gives cooling ages in the range 97-102 Ma [*Grove and Bebout*, 1995]. The depositional age is therefore ~ 10 Ma older than that of the lawsonite and epidote blueschists, and the metamorphic age could also be older, but the Ar-Ar ages leave open the possibility that all the lower grade

289 rocks on Catalina were metamorphosed at about the same time and at similar depths, but at
290 temperatures between 320 and 566°C.
291 The migmatitic metasediments of the Amphibolite Unit yield an MDA of 122±3 Ma [*Grove*
292 *et al.*, 2008], ~20 m.y. older than the MDA of the lawsonite-blueschist facies rocks. U-Pb ages
293 on metamorphic zircon and titanite and Lu-Hf ages on garnet from the high-grade rocks all
294 cluster around 115-112 Ma [*Mattinson*, 1986; *Anczkiewicz et al.*, 2004; *Page et al.*, 2019;
295 *Cisneros et al.*, 2022], suggesting that this was the time of peak-temperature metamorphism.
296 Sm-Nd ages on garnet [*Harvey et al.*, 2021] and Ar-Ar ages on hornblende [*Grove and Bebout*,
297 1995], both from the high-grade blocks, range from 116-108 Ma; and Ar-Ar ages from
298 muscovite in the migmatitic metasediments range from 105-100 Ma. *Harvey et al.* [2021]
299 interpreted the range in Sm-Nd ages as indicating variable timing of metamorphism due to
300 relative motion of the blocks in the subduction channel. Suggested values for the closure
301 temperature of the Sm-Nd system in garnet range from 600 to 900°C [*Culí et al.*, 2022], but the
302 general consensus is that it depends on both grain-size and cooling rate, and that it is lower than
303 the closure temperature for the Lu-Hf system [*Shu et al.*, 2014]. The fact that several of the Sm-
304 Nd ages are younger than Lu-Hf ages on similar rocks, and the similarity of the Sm-Nd garnet
305 and Ar-Ar hornblende age ranges, suggest that the Sm-Nd ages indicate progressive cooling after
306 peak metamorphism. Cooling continued down to the closure temperature of Ar in muscovite at
307 ~100 Ma, about the time the Ar system closed in the lower grade rocks.

308 **7. Discussion**

309 The sequence of peak temperature conditions on Catalina clearly forms a quasi-continuous
310 inverted sequence from 327°C to ~750°C (Figures 2 and 4). The pressures associated with the
311 peak temperatures are broadly similar, as might be expected if they formed in an inverted
312 temperature gradient at depth in the subduction zone. The high-grade rocks reached peak
313 temperature at ~115 Ma, however, which is 15 m.y. before deposition of the lawsonite-blueschist
314 facies metasediments. Hence the present inverted grade structure does not represent a primary
315 temperature inversion. *Dong et al.* [2022] suggest that the high-grade metamorphism was a
316 result of flow of mantle wedge material up the subduction zone in response to trench retreat, and
317 the ultramafic rocks at the top of the sequence may represent the remains of this material. In that

318 case, there presumably was an inverted temperature gradient at the time of the high-grade
319 metamorphism, but the present sequence of rocks does not directly reflect that.
320 The Ar-Ar data from the lower grade rocks are permissive of the possibility that they were
321 metamorphosed at about the same time (~100 Ma), and hence formed in an inverted temperature
322 gradient, presumably with the higher grade rocks above as a heat source. A more plausible
323 alternative may be that they formed by the progressive underplating of rocks in a cooling
324 environment, following the 115 Ma high-T event [e.g., *Cooper et al.*, 2011]. In this case, the
325 present inverted sequence is entirely constructional, although an inverted temperature gradient
326 would have existed for the 15-20 m.y. duration of this history.
327 Can we place limits on the magnitude of this inverted gradient? Seismic data suggest that
328 active subduction channels at the present day are close to the limit of resolution, i.e., not more
329 than 5 km thick [*Calvert*, 2004]. The peak temperature at the upper boundary of the channel was
330 ~750°C (Amphibolite Unit). We can estimate the temperature at the bottom of the channel (the
331 top of the down-going slab) to have been ~250°C at 50 km depth, based on thermal modeling
332 estimates of the temperature of the slab top in the absence of shear heating (e.g., *Syracuse et al.,*
333 2010). This suggests that the average inverted gradient within the subduction channel at the time
334 of the high-grade metamorphism might have been ≥100°C/km.
335 The gradient would have declined with time, as younger rocks were emplaced beneath the
336 high-grade rocks. Our temperature data are not precise enough to estimate gradients within the
337 slices, but the present sequence is not more than ~700 m thick at maximum, and there are jumps
338 in temperature of ~100°C or more across each of the tectonic contacts between the various slices.
339 The lack of any blueschist facies overprint in the Amphibolite Unit suggests that it was
340 juxtaposed with the lowest grade rocks at pressures of < 7 kbar (equivalent to ~ 26 km depth).
341 Hence the tectonic contacts between the units not only cut out much of the original inverted
342 sequence, but they contributed to exhumation during this process (in effect this means that the
343 faults are low-angle normal faults, rather than thrusts). We can therefore envisage a situation
344 where albite-epidote amphibolite facies rocks, underplated and metamorphosed at > 36 km
345 depth, were subsequently juxtaposed against upper amphibolite facies rocks at a depth of < 26
346 km across a normal-sense fault with a vertical component of displacement of ~10 km (blue line
347 in Figure 5, 105 Ma panel). Epidote blueschist facies rocks and subsequently lawsonite

blueschist facies rocks were each underplated at depths of ~ 36 km, and progressively exhumed and emplaced below the higher grade rocks across similar normal-sense faults.

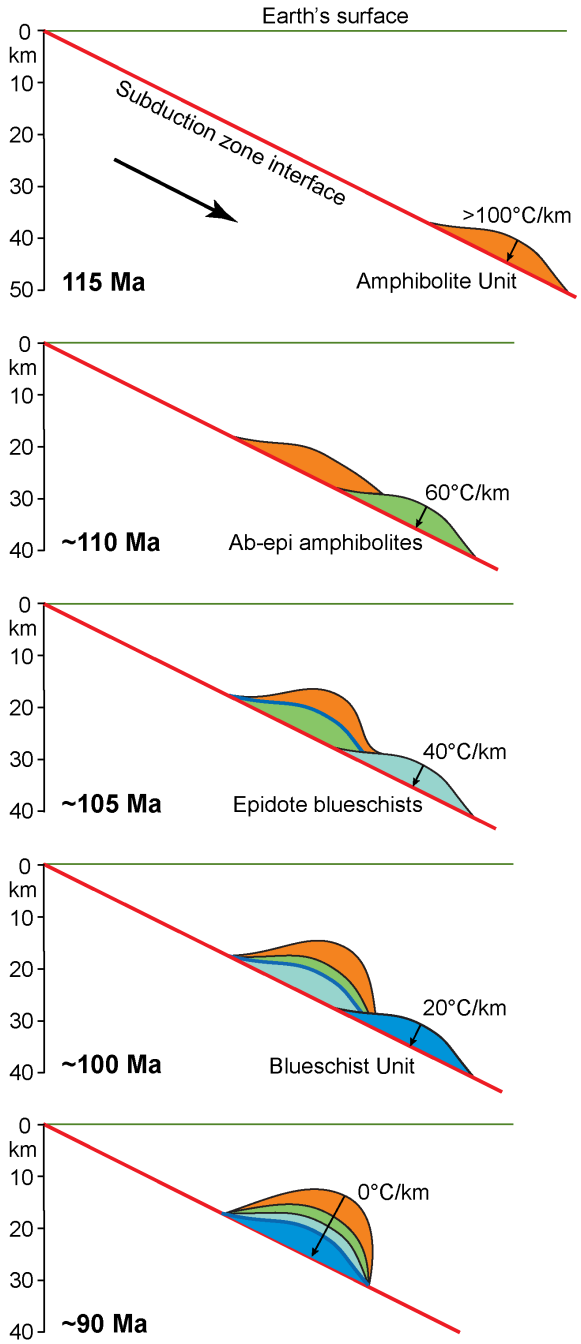

Figure 5. Sequential evolution of the inverted metamorphic grade sequence on Catalina Island. The dip of the subduction zone megathrust (red line) is kept arbitrarily constant, and the geometry of the underplated units is schematic. The upper contact of each of the lower-grade units is an exhumation-

related normal-sense fault (blue lines). A likely value for the true inverted temperature gradient is shown for each step, based on the observed metamorphic temperatures, a 5 km thick subduction channel beneath the megathrust, and a temperature of 250°C at the top of the subducted slab.

During underplating, each accreted slice in turn occupies the top of the subduction channel, and the thermal gradient between it and the bottom of the subduction channel can be estimated based on its peak metamorphic temperature. Inverted temperature gradients within the intermediate and lower grade units estimated in this way were likely in the range 60-10°C/km. By 90 Ma the gradient would have declined to about zero. This evolution was accomplished by a combination of simultaneous subduction, underplating and exhumation. Exhumation was likely a result of return flow up the subduction channel, driven either by buoyancy [*Gerya and Stöckhert*, 2002; *Beaumont et al.*, 2009; *Behr and Platt*, 2013] or topographic loading [*Xia and Platt*, 2017], together with underplating plus extension in the accretionary wedge [*Platt*, 1986].

8. Conclusions

New temperature data from the Catalina Schist Terrane confirm the existence of a quasi-continuous inverted temperature sequence from 327°C to ~750°C in rocks metamorphosed at 35-50 km depth in the late Cretaceous subduction zone on the western margin of North America. The highest grade rocks were metamorphosed ~20 m.y. before the lowest grade rocks, however, so the inverted grade structure does not directly represent a primary temperature inversion. The rocks were progressively underplated and exhumed in a cooling environment following a high-T metamorphic event at 115 Ma, possibly caused by flow of mantle wedge material up the subduction zone in response to trench retreat. An inverted temperature gradient of ≥100°C/km is likely during the high-T event, which decreased during successive underplating of the intermediate and lower grade rocks, and reached zero by ~90 Ma.

Acknowledgements

Reviewers and editors. We thank Aaron Celestian for allowing us to use the laser Raman facilities at the Natural History Museum of Los Angeles. This research did not receive any specific grant from funding agencies in the public, commercial, or not-for-profit sectors.

Open Research

Data Availability Statement.

386 The data on which this research was based has been deposited in the EarthChem Data
387 Repository, and can be accessed at the following URL: https://doi.org/10.26022/IEDA/112994.
388 Please cite these data as Platt, J., Schmidt, W., 2023. Laser Raman analysis of carbonaceous
389 material, Catalina subduction complex, California, Version 1.0. Interdisciplinary Earth Data
390 Alliance (IEDA). https://doi.org/10.26022/IEDA/112994. Accessed 2023-07-20. The data consist
391 of a single Excel file that includes sample locations, operational data, and the raw Raman data
392 files used to construct the LRCM spectra.

393 **References**

394 Ammar, M. R., and J. N. Rouzaud (2012), How to obtain a reliable structural characterization of
395 polished graphitized carbons by Raman microspectroscopy, *Journal of Raman spectroscopy*,
396 *43*, 207-211.
397 Anczkiewicz, R., J. P. Platt, M. F. Thirlwall, and J. Wakabayashi (2004), Franciscan subduction
398 off to a slow start: Evidence from high-precision Lu-Hf garnet ages on high-grade-blocks,
399 *Earth and Planetary Science Letters*, *225*, 147-161.
400 Bailey, E. H. (1941), Mineralogy, petrology, and geology of Santa Catalina Island, Stanford
401 University.
402 Beaumont, C., R. A. Jamieson, J. P. Butler, and C. J. Warren (2009), Crustal structure: A key
403 constraint on the mechanism of ultra-high-pressure rock exhumation, *Earth and Planetary*
404 *Science Letters*, *287*(1-2), 116-129.
405 Behr, W. M., and J. P. Platt (2013), Rheological evolution of a Mediterranean subduction
406 complex, *Journal of Structural Geology*, *54*, 136-155.
407 Beyssac, O., B. Goffé, C. Chopin, and J. N. Rouzaud (2002), Raman spectra of carbonaceous
408 material in metasediments: a new geothermometer, *Journal of Metamorphic Geology*, *20*,
409 859–871.
410 Beyssac, O., B. Goffé, J. P. Petitet, E. Froigneux, M. Moreau, and J. N. Rouzaud (2003), On the
411 characterization of disordered and heterogeneous carbonaceous materials by Raman
412 spectroscopy, *Spectrochimica Acta Part A: Molecular and Biomolecular Spectroscopy*, *59*,
413 2267-2276.
414 Calvert, A. J. (2004), Seismic reflection imaging of two megathrust shear zones in the northern
415 Cascadia subduction zone, *Nature*, *428*, 163-167.

Cisneros, M., W. M. Behr, J. P. Platt, and R. Anczkiewicz (2022), Quartz-in-garnet barometry constraints on formation pressures of eclogites from the Franciscan Complex, California, *Contributions to Mineralogy and Petrology*, *177*.

Cooper, F. J., J. P. Platt, and R. Anczkiewicz (2011), Constraints on early Franciscan subduction rates from 2-D thermal modeling, *Earth and Planetary Science Letters*, *312*(1-2), 69-79.

Culí, L., J. Solé, P. Schaaf, G. Solís-Pichardo, J. A. G. Oalmann, and M. Campeny (2022), Sm–Nd isotope whole rock and garnet from the southwestern Grenvillian Oaxacan Complex, Mexico: A review of garnet closure temperature and structural implications, *Journal of South American Earth Sciences*, *119*, 103967.

Dong, J., M. Grove, C. Wei, B.-F. Han, A. Yin, J. Chen, A. Li, and Z. Zhang (2022), Trench retreat recorded by a subduction zone metamorphic history, *Geology*, *50*, 1281-1286.

England, P., and P. Molnar (1993), The interpretation of inverted metamorphic isograds using simple physical calculations, *Tectonics*, *12*(1), 145-157.

England, P. C., and A. J. Smye (2023), Metamorphism and deformation on subduction interfaces: 1. Physical framework, *Geochemistry, Geophysics, Geosystems,* 24, e2022GC010644. https://doi.org/10.1029/2022GC010644.

Ernst, W. G. (1965), Mineral parageneses in Franciscan metamorphic rocks, Panoche Pass, California, *Geological Society of America Bulletin*, *76*, 879-914.

Ernst, W. G. (1993), Metamorphism of Franciscan tectonostratigraphic assemblage, Pacheco Pass area, east-central Diablo Range, California Coast Ranges, *Geological Society of America Bulletin*, *105*, 618-636.

Ernst, W. G., and R. J. McLaughlin (2012), Mineral parageneses, regional architecture, and tectonic evolution of Franciscan metagraywackes, Cape Mendocino-Garberville-Covelo 30′ × 60′ quadrangles, northwest California, *Tectonics*, *31*, TC1001, doi: 10.1029/2011TC002987.

Gerya, T. V., and B. Stöckhert (2002), Exhumation rates of high pressure metamorphic rocks in subduction channels: The effect of rheology, *Geophysical Research Letters*, *29*, 1261, doi:10.1029/2001GL014307.

Graham, C. H., and P. C. England (1976), Thermal regimes and regional metamorphism in the vicinity of overthrust faults: an example of shear heating and inverted metamorphic zonation from southern California, *Earth and Planetary Science Letters*, *31*, 142-152.

447 Grove, M., and G. E. Bebout (1995), Cretaceous tectonic evolution of coastal southern
448 California: Insights from the Catalina Schist, *Tectonics*, *14*, 1290-1308.
449 Grove, M., G. E. Bebout, C. E. Jacobson, A. P. Barth, D. L. Kimbrough, R. L. King, H. Zou, O.
450 M. Lovera, B. J. Mahoney, and G. E. Gehrels (2008), The Catalina Schist: Evidence for
451 middle Cretaceous subduction erosion of southwestern North America, *Geological Society of*
452 *America Special Paper*, *436*, 335-361.
453 Harvey, K., S. Walker, P. Starr, S. Penniston-Dorland, M. Kohn, and E. Baxter (2021), A
454 mélange of subduction ages: constraints on the timescale of shear zone development and
455 underplating at the subduction interface, Catalina Schist (Ca, USA), *Geochemistry,*
456 *Geophysics, Geosystems*, *22*, e2021GC009790, doi. org/10. 1029/ 2021G C0097 90.
457 Harvey, K. M., S. C. Penniston-Dorland, M. J. Kohn, and P. M. Piccoli (2020), Assessing P-T
458 variability in mélange blocks from the Catalina Schist: Is there differential movement at the
459 subduction interface?, *Journal of Metamorphic Geology*, *39*, 271-295.
460 Henry, D. G., I. Jarvis, G. Gillmore, and M. Stephenson (2019), Raman spectroscopy as a tool to
461 determine the thermal maturity of organic matter: Application to sedimentary, metamorphic
462 and structural geology, *Earth Science Reviews*, *198*, 102936.
463 Henry, D. G., I. Jarvis, G. Gillmore, M. Stephenson, and J. F. Emmings (2018), Assessing low-
464 maturity organic matter in shales using Raman spectroscopy: Effects of sample preparation
465 and operating procedure, *International Journal of Coal Geology*, *191*, 135-151.
466 Howell, D. G., and J. G. Vedder (1981), Structural implications of stratigraphic discontinuities
467 across the southern California continental borderland, in *The Geotectonic Development of*
468 *California*, edited by W. G. Ernst, Prentice Hall, Englewood Cliffs, New Jersey.
469 Jamieson, R. A. (1980), Formation of metamorphic aureoles beneath ophiolites: Evidence from
470 the St Anthony complex, Newfoundland, *Geology*, *8*, 150-154.
471 Kouketsu, Y., T. Mizukami, H. Mori, S. Endo, M. Aoya, H. Hara, D. Nakamura, and S. Wallis
472 (2014), A new approach to develop the R aman carbonaceous material geothermometer for
473 low-grade metamorphism using peak width, *Island Arc*, *23*, 33-50.
474 Liou, J. G. (1971), P-T stabilities of laumonite, wairakite, lawsonite, and related minerals in the
475 system CaAlSiO8-SiO- HO, *Journal of Petrology*, *12*, 379-411.
476 Lünsdorf, N. K. (2016), Raman spectroscopy of dispersed vitrinite—Methodical aspects and
477 correlation with reflectance, *International Journal of Coal Geology*, *153*, 75-86.

478 Mattinson, J. M. (1986), Geochronology of high-pressure - low-temperature Franciscan
479 metabasites: A new approach using the U-Pb system. In: Blueschists and Eclogites (Ed.
480 Evans, B.W; Brown, E.H.), *Geological Society of America Memoir*, *164*, 95-106.
481 Mosenfelder, J. L., and B. R. Hacker (1996), Metamorphism and deformation along the
482 emplacement thrust of the Semail Ophiolite, Oman, *Earth and Planetary Science Letters*,
483 *144*, 435-451.
484 Newton, R. C., and G. C. Kennedy (1963), Some equilibrium reactions in the join CaAlSi08-
485 H20, *Journal of Geophysical Research*, *68*, 2967-2984.
486 Newton, R. C., and J. V. Smith (1967), Investigations concerning the breakdown of albite at
487 depth in the earth, *Journal of Geology*, *75*, 268-286.
488 Page, F. Z., E. M. Cameron, C. M. Flood, J. W. Dobbins, M. J. Spicuzza, K. Kitajima, A.
489 Strickland, T. Ushikubo, C. G. Mattinson, and J. W. Valley (2019), Extreme oxygen isotope
490 zoning in garnet and zircon from a metachert block in mélange reveals metasomatism at the
491 peak of subduction metamorphism, *Geology*, *47*, 655-658.
492 Pasteris, J. D. (1989), In situ analysis in geological thin-sections by laser Raman microprobe
493 spectroscopy: a cautionary note, *Applied Spectroscopy*, *43*, 567-570.
494 Peacock, S. M. (1987), Creation and preservation of subduction-related inverted metamorphic
495 gradients, *Journal of Geophysical Research*, *92*, 12,763-12,781.
496 Penniston-Dorland, S. C., M. J. Kohn, and P. M. Piccoli (2018), A mélange of subduction
497 temperatures: Evidence from Zr-in-rutile thermometry for strengthening of the subduction
498 interface, *Earth and Planetary Science Letters*, *482*, 525-535.
499 Platt, J. P. (1975), Metamorphic and deformational processes in the Franciscan Complex,
500 California: Some insights from the Catalina Schist terrane, *Geological Society of America*
501 *Bulletin*, *86*, 1337-1347.
502 Platt, J. P. (1976), The petrology, structure and geologic history of the Catalina Schist terrain,
503 southern California, *University of California Publications in Geological Sciences*, *112*, 1-
504 111.
505 Platt, J. P. (1986), Dynamics of orogenic wedges and the uplift of high-pressure metamorphic
506 rocks, *Geological Society of America Bulletin*, *97*, 1037-1053.
507 Platt, J. P., M. Grove, D. L. Kimbrough, and C. E. Jacobson (2020), Structure, metamorphism,
508 and geodynamic significance of the Catalina Schist terrane, in *From the Islands to the*

509 *Mountains: A 2020 View of Geologic Excursions in Southern California: Geological Society*
510 *of America Field Guide 59.*, edited by R. V. Heermance and J. J. Schwartz, pp. p. 165–195,
511 Geological Society of America.
512 Platt, J.,and Schmidt, W., 2023. Laser Raman analysis of carbonaceous material, Catalina
513 subduction complex, California, Version 1.0 [Dataset]. Interdisciplinary Earth Data Alliance
514 (IEDA). https://doi.org/10.26022/IEDA/112994.
515 Searle, M. P., and J. Malpas (1980), Structure and metamorphism of rocks beneath the Semail
516 ophiolite of Oman and their significance in ophiolite obduction, *Transactions of the Royal*
517 *Society of Edinburgh: Earth Sciences*, *71*, 247-262.
518 Searle, M. P., D. J. Waters, M. W. Dransfield, B. J. Stephenson, C. B. Walker, J. D. Walker, and
519 D. C. Rex (1999), Thermal and mechanical models for the structural and metamorphic
520 evolution of the Zanskar High Himalaya. In: Mac Niocaill, C; Ryan, P.D; eds. Continental
521 Tectonics, *Geological Society of London Special Publication*, *164*, 139-156.
522 Shu, Q., G. Brey, A. Gerdes, and H. Hoefer (2014), Mantle eclogites and garnet pyroxenites –
523 the meaning of two-point isochrons, Sm–Nd and Lu–Hf closure temperatures and the cooling
524 of the subcratonic mantle, *Earth and Planetary Science Letters*, *389*, 143-154.
525 Sorensen, S. S. (1986), Petrologic and geochemical comparison of the blueschist and greenschist
526 units of the Catalina Schist terrane, southern California, *Geological Society of America*
527 *Memoir*, *164*, 59-75.
528 Sorensen, S. S. (1988), Petrology of amphibolite-facies mafic and ultramafic rocks from the
529 Catalina Schist, southern California: metasomatism and migmatization in a subduction zone
530 metamorphic setting, *Journal of Metamorphic Geology*, *6*, 405-435.
531 Sorensen, S. S., and M. D. Barton (1987), Metasomatism and partial melting in a subduction
532 complex Catalina Schist, southern California, *Geology*, *15*, 115-118.
533 Soret, M., P. Agard, B. Dubacq, A. Plunder, and P. Yamato (2017), Petrological evidence for
534 stepwise accretion of metamorphic soles during subduction infancy (Semail ophiolite, Oman
535 and UAE), *Journal of Metamorphic Geology*, *35*, 1051-1080.
536 Syracuse, E. M., P. E. Van Keken, and G. A. Abers (2010), The global range of subduction zone
537 thermal models, *Physics of the Earth and Planetary Interiors*, 183, 73-90.
538 Stuart, C. J. (1979), Middle Miocene paleogeography of coastal southern California and the
539 California borderland: Evidence from schist-bearing sedimentary rocks, in *Cenozoic*

Paleogeography of the Western United States, edited by J. M. Armentrout, pp. 29–44, Society of Economic Paleontologists and Mineralogists, Pacific Section.

Tsujimori, T., and W. G. Ernst (2014), Lawsonite blueschists and lawsonite eclogites as proxies for palaeo-subduction zone processes: a review, *Journal of Metamorphic Geology*, *32*, 437-454.

Vannay, J. C., and B. Grasemann (2001), Himalayan inverted metamorphism and syn-convergence extension as a consequence of a general shear extrusion, *Geological Magazine*, *138*, 253-276.

Wakabayashi, J. (1990), Counterclockwise P-T-t paths from amphibolites, Franciscan Complex, California: relics from the early stages of subduction zone metamorphism, *Journal of Geology*, *98*, 657-680.

Xia, H., and J. P. Platt (2017), Structural and rheological evolution of the Laramide subduction channel in southern California, *Solid Earth*, *8*, 379-403.